

Learning to Assist Drone Landings

Kal Backman, Dana Kulić and Hoam Chung

Abstract—Unmanned aerial vehicles (UAVs) are often used for navigating dangerous terrains, however they are difficult to pilot. Due to complex input-output mapping schemes, limited perception, the complex system dynamics and the need to maintain a safe operation distance, novice pilots experience difficulties in performing safe landings in obstacle filled environments. Previous work has proposed autonomous landing methods however these approaches do not adapt to the pilot’s control inputs and require the pilot’s goal to be known a priori. In this work we propose a shared autonomy approach that assists novice pilots to perform safe landings on one of several elevated platforms at a proficiency equal to or greater than experienced pilots. Our approach consists of two modules, a perceptual module and a policy module. The perceptual module compresses high dimensionality RGB-D images into a latent vector trained with a cross-modal variational auto-encoder. The policy module provides assistive control inputs trained with the reinforcement algorithm TD3. We conduct a user study (n=33) where participants land a simulated drone on a specified platform out of five candidate platforms with and without the use of the assistant. Despite the goal platform not being known to the assistant, participants of all skill levels were able to outperform experienced participants while assisted in the task.

I. INTRODUCTION

Unmanned aerial vehicles (UAVs) have become increasingly popular for reconnaissance and inspection tasks, due to their high mobility in traversing dangerous terrains such as mine shafts and tunnels. In such environments, remotely operated UAVs are preferred over full automation, as it is difficult to fully automate human decision making in the challenging and safety-critical context. However, the high mobility comes at a cost of increased teleoperation complexity. When coupled with poor depth perception from maintaining a safe operation distance and increased disturbances from the ground effect [1], performing a safe landing in obstacle-filled environments becomes an increasingly difficult task for novice pilots. To reduce the associated cost of training pilots and increase the accessibility of UAV piloting to all, we seek to find a method that allows novice pilots to safely land at a performance level equal to or greater than expert pilots.

Previous autonomous landing methods [2]–[5] reduce the difficulty of the task, however these methods rely on knowing the pilot’s goal prior to landing and neglect any form of adaptation with the pilot. Shared autonomy systems address these concerns by combining user inputs with that of artificial intelligence to collaboratively complete tasks. There are two main challenges when implementing a shared autonomy system: (i) predicting what the user’s goal is and (ii) deciding how

to assist the user based on this prediction. In the context of safely landing a drone, there may exist multiple safe landing zones within a given environment. However, conditional on the goals of the pilot, only a subset of these may be suitable. This goal uncertainty is caused by private information from the pilot being unknown to the assistant. Although the pilot could explicitly state these goals through alternate interfaces, prior work suggests that explicit communication leads to ineffective collaboration [6]–[8] compared to implicit means. Inferring implicit information of the pilot’s intent through observations of their actions relative to the environment, the assistant can make a prediction of the pilot’s intended goal in a seamless manner. Once the goal is inferred, the assistant must then decide what degree/type of assistance to provide. Providing insufficient assistance can result in task failure whilst excessive exerted control, albeit following an optimal strategy, leads users to perceive the system as untrustworthy [9].

The previously mentioned challenges of predicting the pilot’s goal and how much control should be exerted are related to the perspective of the assistant, which views the pilot as providing an approximation of the optimal policy that needs to be fine-tuned. From the perspective of the pilot, two challenges exist: (i) the uncertainty in estimating the state of the UAV and (ii) developing a dynamic model that maps control inputs to physical changes of the UAV’s state. For the pilot to successfully land the UAV, they must estimate the relative position of the UAV to that of the landing target. Estimation of the UAV’s depth is challenging for pilots, as it is inferred from the perceived size of the UAV, whereas estimation of the UAV’s latitude and elevation are based on the projected location within the pilot’s view plane. This leads to poor depth estimation of the UAV and the resultant actions taken by the pilot being misaligned with the intended goal. To successfully operate the UAV, pilots must develop an internal dynamic model that maps control inputs to state transitions. This mapping and dynamic model is developed through accumulated interactions with the environment and is a result of the pilot’s experience.

A. Problem statement and model overview

Our goal is to develop an assistive system that allows novice pilots to land a UAV on one of several platforms at a proficiency greater than or equal to that of an experienced pilot. We define an experienced pilot as one that can accurately estimate the position of the UAV and reliably land on the centre of a given platform. To control the drone the pilot provides target linear XYZ velocities for the on-board flight controller to follow. The pilot is aware of the desired landing platform but due to maintaining a safe distance, has difficulty

Authors are with the Department of Electrical and Computer Systems Engineering and the Department of Mechanical and Aerospace Engineering, Monash University. [Kal.Backman1, Dana.Kulic, Hoam.Chung]@monash.edu.

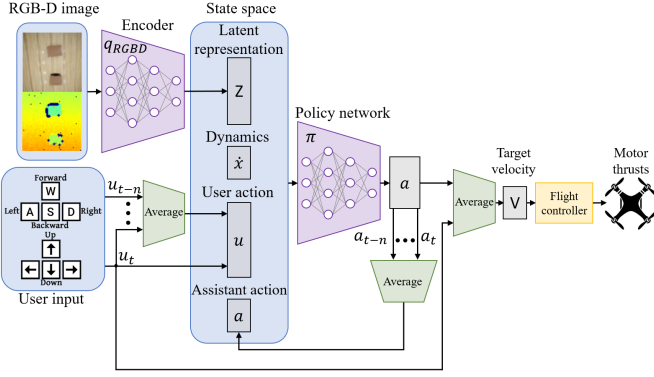


Fig. 1: System architecture used to assist pilots in landing. Encoder q_{RGBD} takes an RGB-D image as input and creates a compressed latent representation. The latent representation is then fed into the policy network along with other state variables from which an action is generated. The resultant action is then averaged with the pilot's action to create a target velocity for the flight controller.

in perceiving the depth of the UAV. On the other hand, the assistant understands the control inputs required for a successful landing however it is unaware of the pilot's goal which must be inferred from observations of the pilot's commands to the UAV during interaction with the environment.

Our approach is summarised in Fig. 1 and is comprised of two components: (i) learning a compressed latent representation of the environment to perceive the location and structure of the landing platforms and (ii) learning a policy network to provide control inputs to assist the pilot in successful landing. The first component takes noisy RGB-D data from a downwards facing camera attached to the UAV and encodes information of the scene and landing platform location into a low-dimensional latent vector representation. The second component takes the latent vector, UAV dynamics, pilot input and the network's previous average action as input to output a target velocity for the UAV. The UAV's final target velocity is determined by averaging the action of the pilot and that of the network which is then fed into the flight controller.

B. Related work

Common fully autonomous landing methods use visual servoing [10] to approach a predefined target. The limitations of such an approach is that the target must remain in the camera's field of view throughout the task. Model-based approaches are favoured for moving platform tasks [3], [5] due to alleviating the need of continual visual observations by predicting the motion of the UAV and target. Both approaches require that a single unambiguous landing zone exists and is of a predefined shape, making them unsuitable for unstructured environments. Our approach aims to address these concerns by training over a wide variety of landing zones where multiple potential landing zones exist within a single environment.

Learning based approaches as seen in [2], [4] use deep neural networks to learn the necessary control inputs required

for a successful landing. [2] uses a hierarchy of deep Q-learning networks (DQNs) to learn an end-to-end mapping from input RGB images to output action velocities for the UAV to follow. The network was able to learn to detect and land on observed targets however due to the large state-space from end-to-end mapping, the policy required two separate DQNs to manage the detection and landing phase independently. By learning from a latent representation in our proposed approach, a single policy network is required due to the increased sample efficiency of the learning process.

The previously mentioned autonomous landing approaches fulfill their intended purpose however lack the ability to handle multiple potential landing zones and are not adaptive to pilot inputs. Previous shared autonomy systems [11]–[13] facilitate user adaptability and handle unknown goals however require either a known dynamic model of the world, a set of known potential goals or a set of predefined user policies. These constraints limit the practicality of implementing such approaches due to the difficulty associated in developing accurate dynamic models and the requirement to pre-define the position of potential landing sites beforehand. Reddy et al. [14] use shared autonomy to demonstrate a model-free approach using deep Q-learning to assist pilots landing in the lunar lander game. The policy network is unaware of the pilot's goal, which is inferred from observations of the environment and the pilot's actions. The drawback of deep Q-learning is that the agent has access to a discrete set of actions which hinders the ability to provide fine control inputs required for safe landing. Instead we propose to implement a policy-gradient reinforcement learning approach to facilitate continuous action space control.

Reddy et al. [14] deploy their DQN to a physical UAV landing user study, however the number of participants ($n=4$) is limited and the landing pad location is included in the state space for the DQN. Sa et al. [15] implement shared autonomy for UAV pole inspection tasks, using a reduction in task space controls to constrain the motion of the UAV. The task is made easier for novice pilots by reducing the controllable degrees of freedom so that the UAV is forced to move concentric to the pole whilst automatically controlling the yaw so that the camera is directly facing the inspected pole. Our proposed work is one of the few published works introducing shared autonomy to UAV landing.

II. LEARNING LATENT SPACE REPRESENTATION – CROSS-MODAL VARIATIONAL AUTO-ENCODER

The purpose of latent space learning is to reduce the time required for the policy network to reach convergence. As the policy network gathers observations in real time, it is costly to explore large state spaces, therefore a reduction in the dimensionality of the state space leads to accelerated convergence [16]. Desired characteristics of a dimensionality reduction technique is that it is smooth, continuous and consistent [17], so that a policy network can efficiently learn how to perceive the encoded environment.

[17] introduces a cross-modal variational auto-encoder (CM-VAE) which trains a latent vector representation from multiple data sources. Given a data sample x_k where k represents the modality such as a RGB image or an arbitrary sensor reading, the encoder q_k transforms x_k into a vector of means μ and variances σ^2 of a normal distribution, from which the vector z is sampled, i.e. $z \sim \mathcal{N}(\mu, \sigma^2)$. The decoder p_l takes the latent sample z and reconstructs to the desired modality l which is denoted as y_l . As the encoder q_k maps the input onto a distribution, a regularizing term is required to ensure that the properties of the desired distribution are met. The Kullback-Leibler divergence is used so that the distribution q_k maps to a normal distribution of $\mathcal{N}(0, 1)$. Traditional VAEs achieve encoding onto a distribution by maximising the variational lower bound on the log-likelihood of the data as seen in [18]. The loss is re-derived in [17] for the CM-VAE to take into consideration different modalities.

A. CM-VAE implementation

Our implementation of CM-VAE architecture is based on the work of [19] which uses a CM-VAE to reconstruct RGB images of gates and their pose parameters from a UAV. Our implementation contains a single input modality from a noisy RGB-D camera, denoted as $x_{RGBD} = [x_{RGB}, x_D]$, and two output modalities in the form of a depth map and relative pose of the closest visible landing pad, denoted as \hat{y}_D and $\hat{y}_{XYZ} = [\hat{X}, \hat{Y}, \hat{Z}]$ respectively. Similar to [19], we use DroNet [20] for the encoder q_{RGBD} , which is equivalent to an 8-layer ResNet [21]. Decoder p_D takes the full latent space vector z i.e. $\hat{y}_D = p_D(z)$, whereas reconstructing y_{XYZ} we use three independent decoders p_X , p_Y and p_Z , each taking a single element of the first three elements of the latent space vector z i.e. $\hat{X} = p_X(z_{[0]}), \hat{Y} = p_Y(z_{[1]})$ and $\hat{Z} = p_Z(z_{[2]})$.

To generate data to train the network we use the AirSim [22] Unreal engine plugin to capture RGB-D images of generated scenes. Each generated scene consists of five identical landing platforms that are aligned along the longitudinal direction with random spacing between them. The platform's width, length and height are generated from a uniform distribution and then each platform is independently shifted and rotated about the yaw axis. Textures are then applied to the platforms, walls and floor from a total of 52 unique materials. A virtual camera is swept through the scene using a bounded random walk process where 50 RGB-D images and relative landing platform locations are recorded before a new scene is generated.

The depth images provided by AirSim are free of noise and imperfections which is not indicative of real-life sensors. Therefore, a noise generating function G is used to create training data, $x_D = G(y_D)$. Noise generating function G consists of four types of noise: normally distributed noise from sensor inaccuracies, salt and pepper noise from feature triangulation mismatch, missing depth values around edges from occlusion and missing depth values in the form of blobs that mimic reflective materials and harsh lighting conditions. RGB image data is included in the encoder input x_{RGBD} despite the decoder p_D reconstructing only the depth of the

scene so that the true depth y_D can be recovered using complimentary RGB information. Our implementation differs from [19] as the objective of our CM-VAE is to not identically reconstruct the input but to reconstruct a denoised version of the input, making our model a denoising CM-VAE.

To train the network, we follow Algorithm 1 outlined in [17] where we have three losses: (i) MSE loss between the true depth map and reconstructed depth map (y_D, \hat{y}_D) , (ii) MSE loss between the true relative landing platform parameters and the estimated parameters (y_{XYZ}, \hat{y}_{XYZ}) and (iii) Kullback-Leibler divergence loss. The total loss is the sum of the three weighted MSE losses where the weights for (y_D, \hat{y}_D) , (y_{XYZ}, \hat{y}_{XYZ}) and KL loss are 1, 2 and 4 respectively. For every input sample x_{RGBD} , there is a corresponding true output sample for each of the modalities, therefore for each training iteration the weights of q_{RGBD} , p_D , p_X , p_Y and p_Z are updated. Results of the training process will be presented in Section V-A.

III. POLICY LEARNING - TD3

The aim of the policy network is to assist the pilot in landing on the desired landing platform by outputting a target velocity for the UAV that is combined with the user's current input. [12] formalizes shared autonomy systems to be modelled as a partially observable Markov decision process (POMDP) by treating the user's goal as a hidden state that is only known by the user and must be inferred by the agent. We define our problem as a POMDP where the set of all possible states is denoted as \mathcal{S} . The pilot's action is part of the current state s . The set of actions the agent can take is denoted as \mathcal{A} . We define the state transition process as a stochastic process, due to the uncertainty in predicting UAV dynamics from turbulence caused by the ground effect, as $T : \mathcal{S} \times \mathcal{A} \times \mathcal{S} \rightarrow [0, 1]$. The reward function is defined as $R : \mathcal{S} \times \mathcal{A} \times \mathcal{S} \rightarrow \mathbb{R}$, the set of observations as Ω with the observation function $\mathcal{O} : \mathcal{S} \times \Omega \rightarrow [0, 1]$ and discount factor $\gamma \in [0, 1]$. Given an optimal policy $\pi : \mathcal{S} \times \mathcal{A}$ that maximises the expected future discounted reward of the Bellman equation

$$Q^\pi(s, a) = R(s, a, s') + \gamma E[Q^\pi(s', a')], \quad (1)$$

the goal of reinforcement learning is to find the closest approximation of the optimal policy.

To approximate the optimal policy, we implement the reinforcement algorithm TD3 [23] as it allows for a model-free continuous action space control whilst addressing the instability concerns of its predecessor DDPG [24]. TD3 is an off-policy actor-critic method that uses double Q-Learning [25] by taking the minimum value between two critics in estimating the Q-value for the next state action pair. Clipped noise is added to the target actor's action to smoothen the estimated Q-value around the action given a state. The full algorithm is described in Algorithm 1 in [23].

A. TD3 implementation

To train the agent we utilize AirSim as our simulation environment for modelling of UAV dynamics. We generate

a scene containing a total of five potential landing platforms aligned longitudinally with random positions within a confined boundary. As training reinforcement learning algorithms takes substantial time, we developed a simulated user instead of human participants for use in training. The simulated user models several behavioural flight and landing styles including attempting to land on incorrect adjacent landing platforms before correcting itself. For each landing sequence, the simulated user is given an initial estimate of where it believes the true goal G is, which is denoted by \hat{G} . We characterise a simulated user with two parameters $\alpha \in [0, 1]$, which describes the simulated user's conformance to the agent's actions and $\beta \in [0, 1]$, a measure of the user's skill which is the ability to improve its own estimate of the goal. Both α and β affect the simulated user's current estimate of the goal position by:

$$\hat{G}_{i+1} = \hat{G}_i + \alpha \frac{a}{K_\alpha} + \beta \frac{G - \hat{G}_i}{K_\beta}, \quad (2)$$

where a is the action taken by the agent and K_α and K_β are both scaling constants.

For each iteration, the agent receives the mean latent space vector from the encoder q_{RGBD} , the UAV dynamics, the simulated user's current action and the average user and agent actions from the previous 1 second interval. The action taken by the agent is a vector in \mathbb{R}^3 which is averaged with the user's input u given that the agent's action has a magnitude greater than 0.25. We ignore small actions taken by the assistant to allow the assistant to relinquish control to the pilot. The resultant vector V_t is the target velocity vector which the UAV should follow.

$$V_t = \begin{cases} \frac{u+a}{2} & \text{if } |a| > 0.25 \\ u & \text{else} \end{cases} \quad (3)$$

To emulate disturbances from general turbulence and the ground effect, we add normally distributed noise to the UAV's target velocity where the variance of the noise is dependent on the distance to the ground. By adding noise to the UAV's target velocity, the simulated user and agent will experience uncertainty in state transitions which better reflects real world control of UAVs. We implement an Ornstein–Uhlenbeck process [26] for exploratory noise which is added to the action taken by the agent and is decayed after successive landings.

Our reward function utilizes three different rewards: (i) the landing distance of the UAV to the centre of the goal platform, (ii) the difference between the distance to the true goal for the current state s_i and the previous state s_{i+1} , given that the distance between the true goal and s_{i+1} is below a threshold and (iii) the magnitude of the action taken by the agent. To take advantage of the off-policy approach we load the experience replay buffer with previously collected state action transitions from previous models. We use a learning rate for the actor and critic of $1e-3$, discount factor of 0.99, batch size of 100 and a target actor and critic update rate of 0.01. Results of the training process will be shown in Section V-B.

IV. USER STUDY

To assess the performance of the network for users of varying skill levels, we conducted a user study where participants performed the task in a simulated environment. The user study was conducted remotely in an unsupervised manner where participants accessed the simulated environment through a web browser of their choice. Participants were first shown an introductory video that explained the task and how the study would operate. The task assigned to participants was to land the simulated drone on one of five platforms in the environment. Participants could move the drone using the W-A-S-D keys for latitude and longitudinal control and the up and down arrows for elevation. To control for the difference in difficulty from randomly generated scene parameters such as lighting and platform size, each participant performed the task using an identical environment which can be seen in Fig. 2. Participants were permitted to perform a maximum of 14 practice landings to understand the requirements of the task and control scheme. During the practice landings the goal platform was randomly assigned, and participants were given feedback after each landing by displaying their relative position to the landing platform. Participants were then assigned to perform the task either unassisted or assisted based on their participant ID number. Each participant was instructed to perform a total of 16 landings in a predefined sequence where no feedback about their performance was given. After completing the initial 16 landings, participants were given a system usability scale (SUS) survey [27] to assess the mode they just completed. The task was then repeated using the same predefined landing sequence but for the opposite mode of flying which was again followed by the SUS survey. After completing all tasks the participants were then asked to fill out the concluding survey which comprised of twenty-one questions. Seven questions related to the participant's experience in piloting physical drones and video games whilst the other fourteen questions queried the participant's perception of the task. The full list of questions can be observed in Table. II & III in Section V-C.

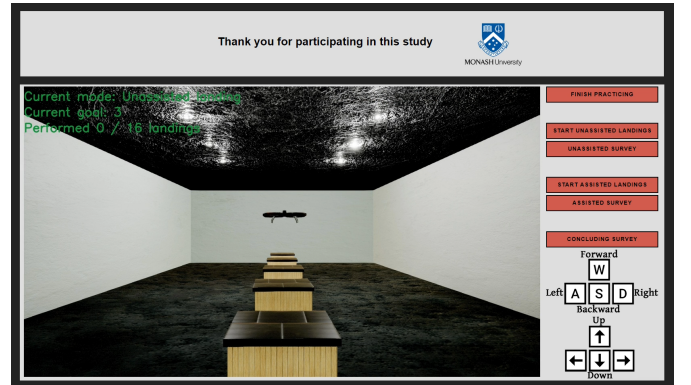


Fig. 2: Example of a participant performing the study in their web browser.

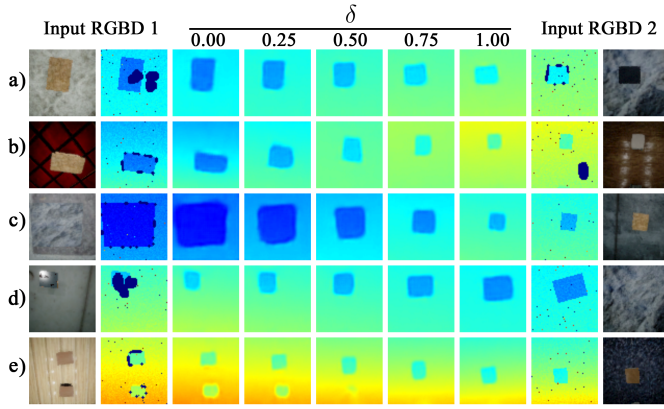


Fig. 3: Visualisation of latent space reconstruction by interpolating between two reference RGB-D images.

V. RESULTS

A. CM-VAE results

The model was trained from a dataset of 50k examples of 64×64 RGB-D images. A separate 10K RGB-D images are used for validation to demonstrate the interpolation of latent space variables and evaluate scene reconstruction. The RMSE error for reconstructing the depth map was 0.1068m while the RMSE error for the individual X , Y & Z parameters are 0.0242m, 0.0282m & 0.0237m respectively.

Fig. 3 shows the reconstruction of linearly interpolated latent vectors using the encoder’s mean vector from two separate RGB-D images. The decoder’s input vector is determined by $\mu_i = \mu_1 + \delta(\mu_2 - \mu_1)$ where μ_1 and μ_2 represent the mean vector from the encoder of image 1 and image 2 respectively. Image pairs a), b) and c) demonstrate the ability to interpolate between simple geometric transformations due to changes in the landing platform shape and relative position. Image pair d) demonstrates the ability to reconstruct the scene under harsh conditions where input image 1’s depth map is degraded with missing depth values around the landing platform, forcing the encoder to utilize RGB information to recover the depth. Input image 2 in image pair d) shows the alternate case where relying on RGB information is unreliable due to the landing platform and the floor’s texture being identical. Image pair e) displays the ability to smoothly transition from states with large differences, where input image 1 contains multiple landing platforms whilst input image 2 has a single landing platform.

B. TD3 simulation results

To quantify the level of assistance provided by the assistant, an experiment was run where a simulated user piloted the UAV for incremental β values. The simulated user performed 40 landing sequences for each β value where β was increased in 0.05 increments at an α value of 0.5. The experiment was first performed without the assistant and then repeated with the assistant. The results of the experiment can be seen in Fig. 4.

Whilst unassisted the simulated user had an average landing error 2.6 times greater than being assisted, while also showing

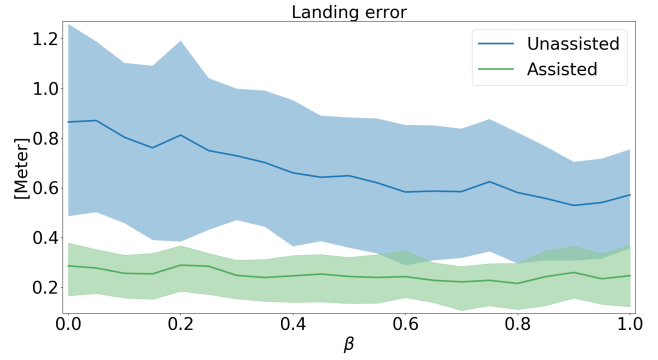


Fig. 4: Performance of the assistant with the simulated user where β acts as a measure of user proficiency.

a greater variability in its performance. Regardless of the simulated user’s skill level, whilst assisted its performance was better than that of a skilled user. The performance of the assistant was also observed to not be affected by the skill of the simulated user. To quantify the agreement between the simulated user and the assistant, we use the time taken to perform the landing sequence normalised by the initial goal distance as a metric. This metric was chosen due to any conflict arising during the flight would cause the average time taken to increase. On average the unassisted simulated user took 2.03 seconds per meter of travel to land where being assisted took 1.94 seconds per meter of travel to land. The marginal difference between the two times shows that the agent does not provide actions that conflict with the simulated user’s goal.

C. User study results

The user study was conducted with the approval of Monash University Human Research Ethics Committee (MUHREC), number 25454. A total of 33 participants completed the user study. The summarised pilot performances can be viewed in Table. I. Participants performed the task with greater proficiency whilst assisted, reducing their median error by over a third and increasing their landing success rate by a factor of three. The performance results are split into two categories based on whether the pilot landed on the instructed platform or to the nearest platform. The error for a given landing is represented as the Euclidean distance of the drone’s centroid to the centre of the platform along the latitude and longitudinal axis. A successful landing is recorded when all four legs of the drone contact the landing platform, while a failure is recorded if the drone falls below a threshold height and not all legs are contacting the platform. Of the 528 unassisted and 528 assisted landings, 10 unassisted landings and 16 assisted landings are excluded from statistical analysis due to the participant immediately landing on the starting platform.

Two-sample statistical tests are performed at a 99% confidence level to test whether a statistically significant difference exists between performing the task unassisted and assisted for a given metric. The test applied to determine a significant difference for the success rate, median error, mean error and variance of the error are the McNemar test, Mood’s median

TABLE I: User study results summary

	Specified platform		Nearest platform	
	Unassisted	Assisted	Unassisted	Assisted
Success rate	26.44%	74.85%	29.50%	93.76%
Median error	1.06m	0.29m	0.88m	0.25m
Mean error	1.35m	1.02m	0.98m	0.28m
Variance	1.24m²	2.33m ²	0.46m ²	0.05m²

Bold values represent a statistically significant difference between the two samples in terms of the most favourable value for the given metric at a significance level of $\alpha = 0.01$.

test, t-test and F-test respectively. A significant difference was found for all metrics tested.

To account for additional effects such as learning and prior experience, a multi-variable regression model is used. The model contains three binary independent variables: (i) whether or not the landing was performed with assistance, (ii) whether or not the landing was performed in the initial half of the study and (iii) whether or not the participant is considered an experienced participant. An experienced participant is defined as one who rated themselves highly in questions 2, 3, 5 and 6 as seen in Table. II. A threshold rating was chosen so that a third of the participants were considered experienced. The binary value associated with human learning (ii) was found to be statistically insignificant at $p = 0.595$, indicating that insufficient evidence exists to infer that participants improved after performing the initial 16 landings. Participant's previous experience (iii) was found to be marginally significant ($p = 0.065$). A significance value of $p < 0.001$ was found for (i) suggesting that whether or not the participant is assisted significantly affected performance whilst controlling for human learning and participant previous experience.

The distribution of pilot errors can be observed in Fig. 5. Whilst flying assisted two distinct modes of errors are formed which coincide with the average distance between landing platforms of 4.0m. Due to the difficulty of the prescribed task, particularly the depth perception, novice pilots often attempted to land in the centre of the valley between platforms. This led to ambiguities in the pilot's goal where the assistant correctly inferred the goal at a rate of 79.34%. Of the correctly inferred goals, 93.34% led to a successful landing.

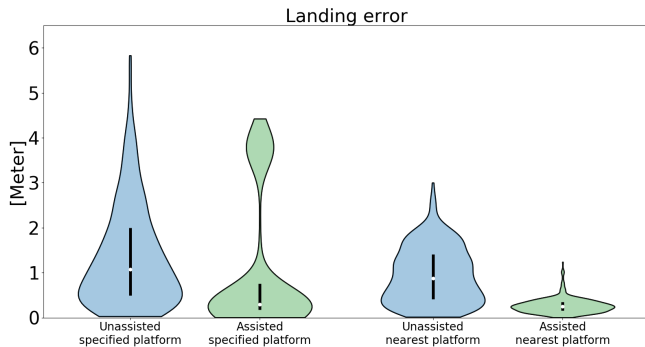


Fig. 5: Violin plot showing the distribution of errors whilst flying unassisted (blue) and assisted (green).

Participants gave an average SUS rating of 60.91 when performing the task unassisted, which falls within the 32nd percentile based on [28]. Assisted participants gave an average SUS rating of 73.41, which corresponds to the 68th percentile, an improvement of the perceived usability of the task by a factor of two. The results of the final survey can be viewed in Table. II & III. Participants preferred performing the task with the assistant as they felt more confident in their ability to accurately land, and perceived the difficulty of the task to be reduced. Participants were also given the opportunity to provide additional feedback about the study; 24 out of 33 participants submitted optional comments.

Out of those who left additional comments, 50% made a remark about the overall difficulty of the task generally pertaining to the lack of depth perception. Further comments of difficulty can be segregated by demographics where those with high gaming experience tended to also complain about graphics and low frame rate while those with piloting experience mentioned difficulties using discrete controls from a keyboard and the lack of audio cues for estimating depth. 21% of those who left comments also mentioned being “not sure what the exact behaviour of the assistance is”. Participants were not provided with information about the methodology of the assistant, causing some participants to believe that the assistant dampened movement whilst landing for finer control or prevented control inputs from being registered when landing where no platform exists.

A further 17% of those who left comments made remarks regarding the inconsistency of the assistant in terms of the degree of assistance provided. It was observed that the assistant would automatically land the drone for the pilot if the assistant was confident about the pilot's goal. However if the assistant was not confident in its estimate of the pilot's goal, the assistant would instead adjust the pilot's input trajectory.

Fig. 6 demonstrates how various skill level participants land the drone. Inexperienced users as shown in Fig. 6 a) tended to have intermittent movement from briefly tapping the movement keys whilst frequently landing near incorrect platforms. Inexperienced participants were also observed to get confused with the control scheme as seen in the right of a) where the participant mistook the fly backwards key for the fly down key. Intermediate participants as shown in b) were able to land in the general vicinity of the landing platform but required assistance to successfully land on the platform. Experienced participants c) reliably landed close to the platforms and only required the assistant for fine movement control. Example trajectory d) shows a failure case of the assistant for an intermediate participant where the participant landed in the centre of the valley between two platforms causing the assistant to take control and land on the incorrect platform.

To quantify the level of assistance provided and to verify if the assistant allows novice users to perform at a level equal to or greater than experienced pilots, we plot each participant's median error against their experience level as shown in Fig. 7. To determine a pilot's experience level, we implement a linear

TABLE II: Final survey - Demographics

1: Have you had any experience with flying a physical drone?	Yes			No	
	45%			55%	
2: How many hours of experience have you with flying physical drones?	0-5	5-10	10-20	20-50	50+
	76%	6%	9%	3%	6%
3: How confident are you with flying physical drones?	Not confident 1	2	3	4	Confident 5
	52%	12%	24%	12%	0%
4: For what purpose have you flown a physical drone for? (Tick all that may apply)	Recreational	Photography Filming	FPV Racing Aerobatics	Inspection	Other
	45%	3%	6%	3%	12%
5: How often do you play video games? (Eg: PC/PS4/Xbox)	Never	Monthly	Weekly	Regularly	Daily
	18%	27%	9%	18%	27%
6: How many hours have you spent on games involving flying?	0-10	10-25	25-100	100-200	200+
	48%	6%	18%	12%	15%
7: When you play video games, what input device do you use? (Tick all that may apply)	Keyboard	Mouse	Hand held controller	Touch screen	Other
	76%	67%	61%	24%	9%

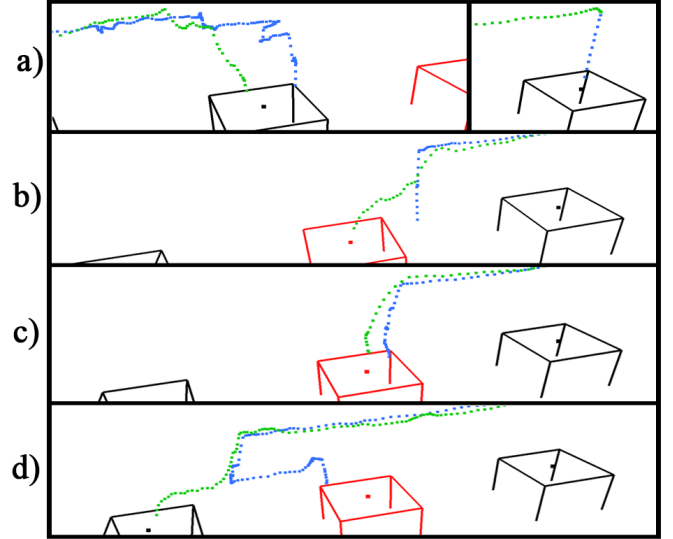


Fig. 6: Trajectories of various participants performing the same landing whilst unassisted (blue) and assisted (green) where the goal platform is denoted in red. Examples a), b) & c) show an inexperienced, intermediate and expert user respectively performing a landing. Example d) demonstrates a failure case for the assistant.

TABLE III: Final survey - User experience

	1	2	3	4	5
8: I felt confident in landing unassisted	21%	42%	15%	18%	3%
9: I felt confident in landing assisted	6%	9%	18%	58%	9%
10: I felt stressed when landing unassisted	9%	18%	27%	39%	6%
11: I felt stressed when landing assisted	24%	36%	21%	15%	3%
12: I felt the task was difficult to perform unassisted	6%	18%	6%	39%	30%
13: I felt the task was difficult to perform assisted	15%	36%	24%	21%	3%
14: I was able to land with greater accuracy whilst being assisted	3%	9%	18%	30%	39%
15: I was able to land quicker whilst being assisted	9%	15%	21%	18%	36%
16: I trust the actions of the assistant	9%	18%	33%	33%	6%
17: The assistant didn't do what I wanted to do	9%	33%	24%	30%	3%
18: I had to fight the assistant for control	18%	36%	15%	12%	18%
19: I prefer to use the assistant when landing	0%	6%	24%	39%	30%
20: I felt being unassisted gave me more freedom	0%	24%	30%	24%	21%
21: I believe that if I practiced, I could perform better without assistance than with assistance	12%	27%	18%	24%	18%

A response of 1 corresponds to strongly disagree whilst a response of 5 corresponds to strongly agree.

regression model that fits the pilot's average landing error as a dependant variable whilst using answers obtained from questions 2, 3, 5 & 6 from the demographic section of the final survey as independent variables. The regressed model provides an estimate of what the predicted mean error should be for a pilot of given experience. The predicted error is normalised between 0 and 1, then inverted so that an experience level of 0 represents a novice whilst an experience level of 1 represents an expert. Fig. 7 shows that whilst assisted, regardless of one's skill level, participants will perform at an equal proficiency that is greater than skilled pilots. Whilst assisted, participant performance was not greatly dependant on their individual skill level which is reflected by a low magnitude regression coefficient of -0.11 compared to that of -0.71 whilst being unassisted. The first author's attempt at the user study is included in Fig. 7, indicated by the yellow highlighted point. This data point is excluded from all statistical analysis but is shown to demonstrate the potential performance of a pilot who has had substantial time to become familiar with the specific setup.

VI. CONCLUSION

In this work we present a shared autonomy approach that allows novice pilots to land a drone on one of several platforms at a proficiency greater than experienced pilots. The approach contains two components (i) an encoder that compresses RGB-D information into a latent vector to facilitate the perception of the physical environment and (ii) a policy network that provides control inputs to assist the pilot with landing. The encoder is trained using a cross-modal variational auto-encoder

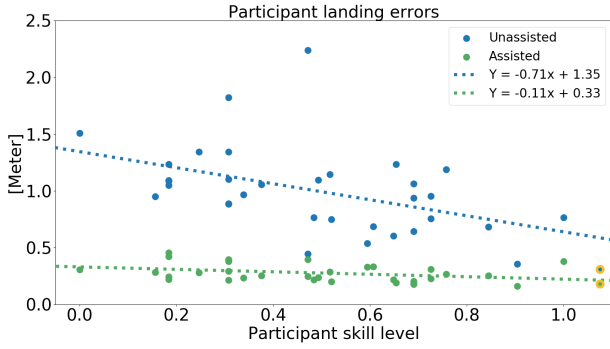


Fig. 7: Plot of participants’ median error for flying unassisted (blue) and assisted (green) against their corresponding skill level. The authors attempt is shown highlighted in yellow and is excluded from all forms of statistical analysis.

which takes noisy RGB-D data and reconstructs a denoised depth map. The policy network is trained within simulation using the reinforcement learning algorithm TD3. We validated our approach by conducting a user study ($n=33$) where participants were tasked with landing a simulated drone on a specified platform from a range of five platforms aligned along the longitudinal axis. Participants achieved significantly higher success rates and lower median and mean errors in the assisted condition, compared to unassisted. Participants also rated the assistant as the preferred mode of performing the task and as more useable. However the success of the assistant landing on the correct platform is limited by the proficiency of the assistant at estimating the true intent of the pilot. Participants also noted that there were issues with the consistency of the degree of assistance provided by the assistant throughout the study. By plotting participants overall performance against skill level as shown in Fig. 7, it can be seen that regardless of skill level, participants will perform better assisted than an unassisted experienced participant, confirming that this approach allows novice pilots to perform at a level greater than or equal to that of experienced pilots.

The authors would like to acknowledge the limitations of the work performed in this paper regarding the absence of physical trials. Due to COVID-19 lockdown restrictions being implemented at the time of this work, it was not feasible to conduct a user study with a physical drone. Future work is planned to integrate the proposed approach onto a physical drone. The encoder will be retrained using a mixture of synthetic and real RGB-D data. Training of the policy network will remain in simulation with modifications to the reward function to heavily penalise landings that may cause damage to the drone. To ensure the safety of participants and drone, we plan to integrate a safety controller that will oversee the physical user study. The planned safety controller will be responsible for monitoring the actions of the assistant and pilot so that the drone does not enter an unrecoverable state that will cause damage to the surroundings. The safety controller will not be used as a method of assistance but as an emergency fail-safe protocol.

REFERENCES

- [1] P. Sanchez-Cuevas, G. Heredia, and A. Ollero, “Characterization of the aerodynamic ground effect and its influence in multirotor control,” *Int. J. Aerosp. Eng.*, vol. 2017, pp. 1–17, 08 2017.
- [2] R. Polvara, M. Patacchiola, S. K. Sharma, J. Wan, A. Manning, R. Sutton, and A. Cangelosi, “Autonomous quadrotor landing using deep reinforcement learning,” *CoRR*, vol. abs/1709.03339, 2017.
- [3] D. Falanga, A. Zanchettin, A. Simovic, J. Delmerico, and D. Scaramuzza, “Vision-based autonomous quadrotor landing on a moving platform,” in *SSRR*, 2017, pp. 200–207.
- [4] G. Shi, X. Shi, M. O’Connell, R. Yu, K. Azizzadenesheli, A. Anandkumar, Y. Yue, and S. Chung, “Neural lander: Stable drone landing control using learned dynamics,” *CoRR*, vol. abs/1811.08027, 2018.
- [5] Y. Feng, C. Zhang, S. Baek, S. Rawashdeh, and A. Mohammadi, “Autonomous landing of a uav on a moving platform using model predictive control,” *Drones*, vol. 2, p. 34, 10 2018.
- [6] M. Goodrich and D. Jr, “Seven principles of efficient human robot interaction,” *IEEE Int. Conf. Syst. Man Cybern.*, pp. 3942 – 3948, 2003.
- [7] D. Vanhooydonck, E. Demeester, M. Nuttin, and H. Brussel, “Shared control for intelligent wheelchairs: An implicit estimation of the user intention,” *ASER*, 01 2003.
- [8] S. Li and X. Zhang, “Implicit intention communication in human–robot interaction through visual behavior studies,” *IEEE Transactions on Human-Machine Systems*, vol. 47, no. 4, pp. 437–448, 2017.
- [9] S. Nikolaidis, D. Hsu, and S. Srinivasa, “Human-robot mutual adaptation in collaborative tasks: Models and experiments,” *The International Journal of Robotics Research*, vol. 36, pp. 618 – 634, 2017.
- [10] Y. Zhang, Y. Yu, S. Jia, and X. Wang, “Autonomous landing on ground target of uav by using image-based visual servo control,” in *36th Chinese Control Conference (CCC)*, 2017, pp. 11 204–11 209.
- [11] S. Nikolaidis, Y. X. Zhu, D. Hsu, and S. S. Srinivasa, “Human-robot mutual adaptation in shared autonomy,” *CoRR*, vol. abs/1701.07851, 2017.
- [12] S. Javdani, H. Admoni, S. Pellegrinelli, S. S. Srinivasa, and J. A. Bagnell, “Shared autonomy via hindsight optimization for teleoperation and teaming,” *Int. J. Rob. Res.*, vol. 37, no. 7, pp. 717–742, 2018.
- [13] Wentao Yu, R. Alqasemi, R. Dubey, and N. Pernalet, “Telemanipulation assistance based on motion intention recognition,” in *ICRA*, 2005, pp. 1121–1126.
- [14] S. Reddy, S. Levine, and A. D. Dragan, “Shared autonomy via deep reinforcement learning,” *CoRR*, vol. abs/1802.01744, 2018.
- [15] I. Sa, S. Hrabar, and P. Corke, “Inspection of pole-like structures using a visual-inertial aided vtol platform with shared autonomy,” *Sensors*, vol. 15, pp. 22003–22048, 2015.
- [16] W. Curran, R. Pocius, and W. D. Smart, “Neural networks for incremental dimensionality reduced reinforcement learning,” in *2017 IEEE/RSJ IROS*, 2017, pp. 1559–1565.
- [17] A. Spurr, J. Song, S. Park, and O. Hilliges, “Cross-modal deep variational hand pose estimation,” *CoRR*, vol. abs/1803.11404, 2018.
- [18] D. P. Kingma and M. Welling, “Auto-encoding variational bayes,” *CoRR*, vol. abs/1312.6114, 2014.
- [19] R. Bonatti, R. Madaan, V. Vineet, S. A. Scherer, and A. Kapoor, “Learning visuomotor policies for aerial navigation using cross-modal representations,” *arXiv: Computer Vision and Pattern Recognition*, 2019.
- [20] A. Loquercio, A. I. Maqueda, C. R. del-Blanco, and D. Scaramuzza, “Dronet: Learning to fly by driving,” *IEEE Robotics and Automation Letters*, vol. 3, no. 2, pp. 1088–1095, 2018.
- [21] K. He, X. Zhang, S. Ren, and J. Sun, “Deep residual learning for image recognition,” *CoRR*, vol. abs/1512.03385, 2015.
- [22] S. Shah, D. Dey, C. Lovett, and A. Kapoor, “Airsim: High-fidelity visual and physical simulation for autonomous vehicles,” *CoRR*, vol. abs/1705.05065, 2017.
- [23] S. Fujimoto, H. van Hoof, and D. Meger, “Addressing function approximation error in actor-critic methods,” 2018.
- [24] T. P. Lillicrap, J. J. Hunt, A. Pritzel, N. Heess, T. Erez, Y. Tassa, D. Silver, and D. Wierstra, “Continuous control with deep reinforcement learning,” *CoRR*, vol. abs/1509.02971, 2015.
- [25] H. V. Hasselt, “Double q-learning,” in *Adv Neural Inf Process Syst 23*. Curran Associates, Inc., 2010, pp. 2613–2621.
- [26] G. E. Uhlenbeck and L. S. Ornstein, “On the theory of the brownian motion,” *Phys. Rev.*, vol. 36, pp. 823–841, Sep 1930.
- [27] J. Brooke, “Sus - a quick and dirty usability scale,” 2006.
- [28] S. Jeff, *A practical guide to the System Usability Scale (SUS)*, 2011.